Protein Assemblies

DOI: 10.1002/anie.201105186

Photocurrent Generation from Hierarchical Zinc-Substituted Hemoprotein Assemblies Immobilized on a Gold Electrode**

*Akira Onoda, Yasuaki Kakikura, Taro Uematsu, Susumu Kuwabata, and Takashi Hayashi**

The creation of efficient electron-transfer interfaces between redox-active proteins and electrodes is a key technological step toward further development of high-performance biosensors and photoelectric conversion biodevices.[1] One of the strategies for wiring the redox-active proteins effectively onto the electrodes is noncovalent immobilization by cofactor reconstitution. Photosynthetic protein complexes,[2] flavoenzymes,[3] and hemoproteins[4] have been successfully coupled to electrodes by using this method. Another promising approach for the enhancement of electron transfer efficiency involves custom-designed fabrication of redox-active protein assemblies on the electrodes.[5]

We recently described the preparation of linear hemoprotein self-assemblies by a specific heme/heme pocket interaction, in which a heme moiety is externally attached to the surface of the H63C single mutant of cytochrome b_{562} (CYT)[6] or A125C single mutant of myoglobin.[7] The supramolecular self-assembling systems of proteins[8] also allowed us to immobilize these assemblies on an electrode surface. Herein we demonstrate the construction of hierarchical assemblies of photoactive hemoproteins connected with the photosensitizing cofactor, namely zinc protoporphyrin IX derivatives (ZnPP),[9] on a gold electrode (Figure 1). This system provides markedly enhanced electrochemical communication relative to a single layer of the protein.

The ZnPPs **1a** and **1b**, which include a maleimide group at the terminus of the one of the heme propionate side chains, were synthesized to introduce the cofactor at the Cys63 residue on the protein surface. Those modified cofactors have different linker lengths between the zinc porphyrin and the protein surface (Figure 1). Coupling of **1a** or **1b** to the H63C mutant was carried out in a buffered solution. The modified protein was denatured with a 6 M guanidine-HCl (Gdn-HCl) solution. The solution was then extracted with 2-butanone to remove the excess ZnPP and the intrinsic native heme, and the separated aqueous layer was dialyzed to remove Gdn-HCl. This process results in the apoprotein modified with ZnPP (ZnPP–apoCYT). The modified protein exhibits characteristic Soret (429 nm) and Q (552 and 592 nm) bands that originate from axial coordination of His and Met residues,[10] thus indicating that the external ZnPP linked onto the protein surface was incorporated into the heme pocket of the protein matrix (Figure S1 in the Supporting Information). The interprotein oligomer of zinc-substituted CYT (ZnPP–apoCYT)$_n$ was successfully prepared in a manner similar to the methods used in our previously reported preparation of a monomer unit with an external heme moiety.[6b,c]

To anchor the protein oligomers on the gold electrode through a ZnPP/heme pocket interaction, a ZnPP-immobilized gold electrode (ZnPP/Au) was prepared by using the reported method with a slight modification:[4a] Firstly, a gold electrode was immersed in a mixed solution of mercaptopro-

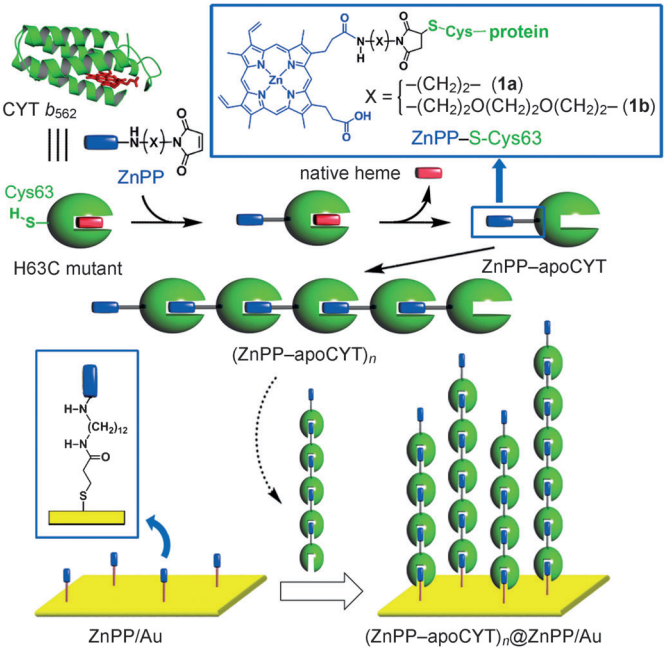

Figure 1. Strategy for immobilization of supramolecular zinc-substituted cyt b_{562} assemblies on the gold electrode.[11] Native heme shown in red, ZnPP in blue, and protein matrices in green.

[*] Dr. A. Onoda, Y. Kakikura, Dr. T. Uematsu, Prof. Dr. S. Kuwabata, Prof. Dr. T. Hayashi
Department of Applied Chemistry
Graduate School of Engineering, Osaka University
2-1 Yamadaoka, Suita, 565-0871 (Japan)
E-mail: thayashi@chem.eng.osaka-u.ac.jp
Dr. A. Onoda
Frontier Research Base for Global Young Researchers
Graduate School of Engineering
Osaka University (Japan)
Prof. Dr. S. Kuwabata
Japan Science and Technology Agency
CREST, Kawaguchi, Saitama 332-0012 (Japan)

[**] This work was supported by Grants-in-Aid for Scientific Research ((B) and Innovative Areas "Coordination Programming", area 2107) from MEXT, the Global COE Program of Osaka University, and the Japan Society for the Promotion of Science (JSPS). A.O. acknowledges a support from the Frontier Research Base for Global Young Researchers, Osaka University, on the Program of MEXT, and from the Ogasawara Foundation. T.H. acknowledges a support from the Asahi Grass Foundation.

Supporting information for this article is available on the WWW under http://dx.doi.org/10.1002/anie.201105186.

pionic acid and 3,3′-dithiobis(propionic acid hydroxysuccinimide ester) with a molar ratio of 5:1 to form the self-assembled monolayer (SAM). Secondly, the electrode was treated with 1,12-diaminododecane, followed by coupling of ZnPP with the terminal amino groups gave the ZnPP-immobilized surface. The increased mass of the electrode was analyzed by using a quartz crystal microbalance (QCM) and confirmed covalent immobilization of ZnPP on the gold surface.[12]

Further immobilization of the modified apoprotein units, ZnPP–apoCYT, onto the ZnPP/Au electrode was evaluated by electrochemical impedance spectroscopy (EIS), which provides sensitive detection of protein binding according to the resistance changes at the electrode–solution interface. The ZnPP/Au electrode was immersed in the protein solution and the unbound proteins in the solution were thoroughly washed away to provide the protein-modified electrodes. The measurements were performed in a buffered solution containing 5 mM $K_4[Fe(CN)_4]/K_3[Fe(CN)_4]$. The charge-transfer resistance R_{CT} for the ZnPP/Au electrode was $0.5\times10^4\ \Omega$, whereas an increased R_{CT} value ($1.3\times10^4\ \Omega$) was observed in the presence of the apoprotein of wild type cytochrome b_{562} ($apoCYT_{wt}$; Figure S2). This result suggests the immobilization of the protein matrices through the ZnPP/heme pocket interactions.[13] Furthermore, much larger resistance values were obtained in the case of (**1a**–apoCYT)$_n$ ($2.1\times10^4\ \Omega$) and (**1b**–apoCYT)$_n$ ($2.3\times10^4\ \Omega$), thus indicating the construction of the integrated assemblies of the zinc-substituted CYT on the gold surface ((ZnPP–apoCYT)$_n$@ZnPP/Au).

QCM measurements were conducted to evaluate the degree of the interprotein assemblies of (**1a**–apoCYT)$_n$ and (**1b**–apoCYT)$_n$ on the ZnPP/Au electrode. Upon addition of $apoCYT_{wt}$, the frequency of the ZnPP-immobilized QCM decreased by 80 Hz (Figure S3). This value is saturated upon the addition of excess $apoCYT_{wt}$, thus showing that the apoproteins occupy the electrode surface. The surface density of the CYT_{wt} matrices was calculated to be 5.4×10^{-12} mol cm^{-2}. In contrast, significant frequency decreases were observed upon the addition of (**1a**–apoCYT)$_n$ (315 Hz) and (**1b**–apoCYT)$_n$ (558 Hz), therefore confirming the accumulation of the ZnPP–apoCYT units on the gold electrode (Figure S3). The average numbers in the protein assemblies of (**1a**–apoCYT)$_n$ ($n=3.9$) and (**1b**–apoCYT)$_n$ ($n=7.0$) indicate that (**1b**–apoCYT)$_n$ with more flexible linker is advantageous for integrating the layer of zinc-substituted CYT.

The electrode surfaces with the protein assemblies in a buffered solution were directly analyzed by atomic force microscopy (AFM) to investigate the detailed morphology (Figure 2). AFM studies showed that the electrode surface of $apoCYT_{wt}$@ZnPP/Au immersed in a buffered solution was fully covered with a single layer of the object of 5 nm in height, which is consistent with the sum of the length for the thiol linker (ca. 2.5 nm) and cyt b_{562} (ca. 2.5 nm; Figure 2a). In contrast, as shown in Figure 2b, we observed significantly higher objects (ca. 20 nm) which show almost perpendicular orientation to the surface on the electrode (**1b**–apoCYT)$_n$@ZnPP/Au, thus suggesting that fibrous protein oligomers were prepared as shown in Figure 1. The average height of the assemblies on the surface is 15.5 nm, which is consistent with that observed by QCM measurements. Such a rigid rodlike alignment of the proteins would be achieved because of the restricted motion of cylindrical CYT protein

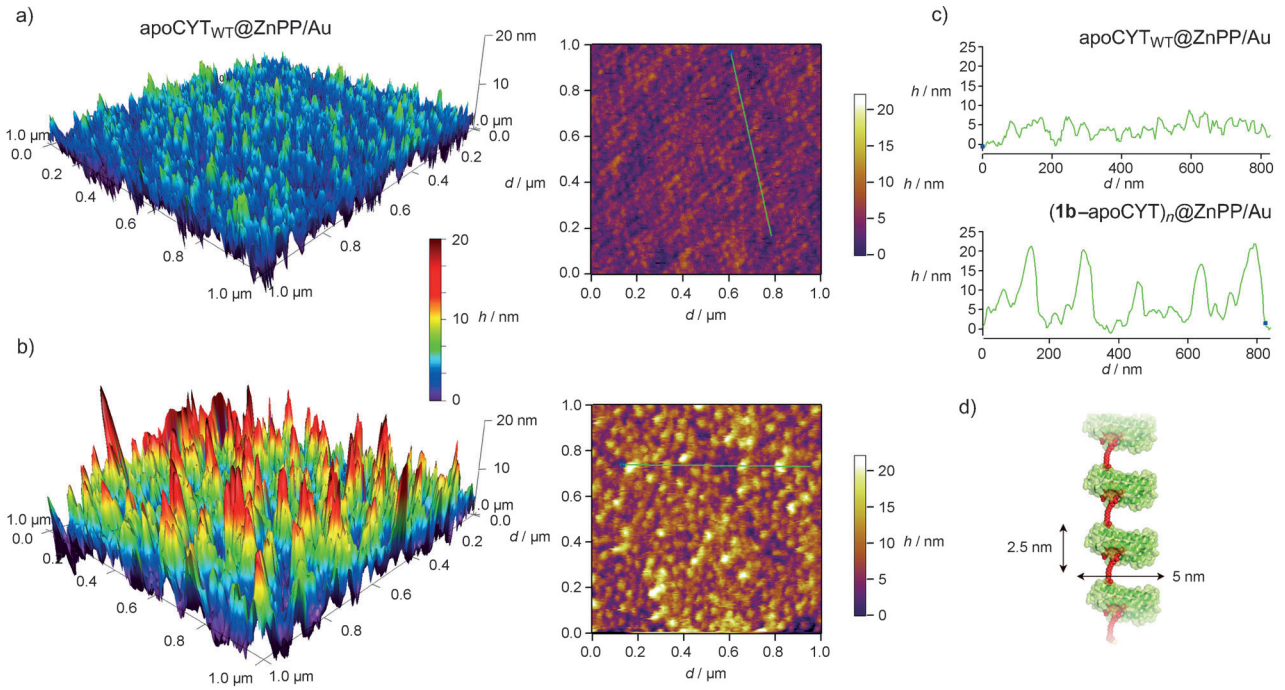

Figure 2. 3D and 2D AFM images of a) $apoCYT_{wt}$@ZnPP/Au and b) (**1b**–apoCYT)$_n$@ZnPP/Au. c) The height profiles in green line in the 2D images of $apoCYT_{wt}$@ZnPP/Au and (**1b**–apoCYT)$_n$@ZnPP/Au. d) Plausible structural model of (ZnPP-apoCYT)$_n$.

units connected with the relatively short linkers at the terminal of the heme propionate side chain (Figure 1).

Photocurrent measurements of $(ZnPP–apoCYT)_n$@ZnPP/Au employed as a working electrode were carried out to investigate the properties of the hierarchical hemoprotein assemblies containing the photosensitizer. Figure 3 shows photocurrent response patterns of the prepared

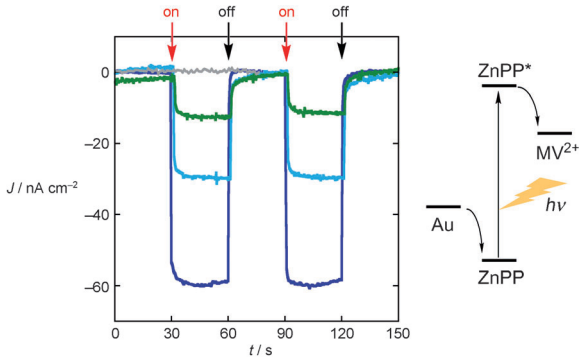

Figure 3. Photocurrent response patterns of $(\mathbf{1a}–apoCYT)_n$@ZnPP/Au (light blue), $(\mathbf{1b}–apoCYT)_n$@ZnPP/Au (blue), and $apoCYT_{wt}$@ZnPP/Au (in green) during on/off cycles of white light. Gray profile shows the background photocurrent of the Au electrode only with SAM. Conditions: 50 mM Tris-HCl (pH 7.5; Tris = tris(hydroxymethyl)aminomethane), methyl viologen (1 mM), bias potential of −200 mV (vs. Ag|AgCl).

electrodes during on/off cycles of white light in the presence of methyl viologen (MV^{2+}) as an electron acceptor. We observed the clear rise and fall of the cathodic current under the bias potential of −200 mV (vs. Ag|AgCl).[14] The action spectra of $(ZnPP–apoCYT)_n$@ZnPP/Au showed characteristic peak maxima that correspond to the Soret and Q bands, respectively (Figure S4). This observation is a strong indication that the photocurrent originates from the photoexcitation of ZnPP within the protein, followed by the reduction of MV^{2+}. When $apoCYT_{wt}$@ZnPP/Au was irradiated with monochromatic light at 420 nm (0.043 mW), we observed a photocurrent response of 13 nA cm^{-2}, whereas the photocurrents of $(\mathbf{1a}–apoCYT)_n$@ZnPP/Au (30 nA cm^{-2}) and $(\mathbf{1b}–apoCYT)_n$@ZnPP/Au (60 nA cm^{-2}) were significantly increased.[15] These findings support the fact that more densely layered assembly of the zinc-substituted proteins on the electrode surface effectively enhances the photocurrent generation.

In conclusion, the construction of zinc-substituted hemoprotein assemblies on the gold electrode by a specific noncovalent ZnPP/heme pocket interaction provides a novel strategy for development of a programmed integration of biomolecules. This work indicates that the fabricated supramolecular assemblies of a photoactive protein on an electrode show a great potential for increasing photoelectric conversion using biodevices. Efforts to expand the attractive features of hemoprotein matrices as electron transfer mediators, sensors, and catalysts through this strategy are now in progress.

Experimental Section

Electrochemical measurements were recorded with a potentiostat (CompactStat, Ivium Technologies) using a platinum wire as a counterelectrode and a standard Ag|AgCl reference electrode. The electrolyte was 100 mM MOPS buffer (pH 7.0) containing 5 mM $K_4[Fe(CN)_4]/K_3[Fe(CN)_4]$.

Quartz crystal microbalance (QCM) measurements were performed using a cell equipped with a 27 MHz QCM plate oscillating at the fundamental frequency. The ZnPP-immobilized QCM cell was filled with a buffered solution (10 mM KPi, pH 7.0, 500 μL), and the time course frequency changes were observed upon the addition of the protein solution (4 μM $(\mathbf{1a}–apoCYT)_n$, $(\mathbf{1b}–apoCYT)_n$, and $apoCYT_{wt}$).

The zinc-substituted hemoprotein assemblies were constructed on the Au(111) electrode surface on the quartz slide, AuroSheet-(111) K. After the electrode surface was immersed with a drop of a fresh buffered solution (50 mM Tris-HCl, pH 7.5), the electrode was gently rinsed with the buffer. AFM images were acquired in AC mode with an Asylum Research MFP-3D-SA microscopy using a SiN_4 tip (Olympus micro cantilever AC40TS with a radius of 10 nm and a spring constant of 0.1 N m^{-1}). The images were taken at room temperature with the line scan speed of 0.5 Hz and 256 pixels per line.

Photocurrent measurements were performed in a typical three-electrode configuration connected to a potentiostat (CompactStat, Ivium Technologies). The protein-modified gold electrode, as a working electrode, was mounted at the cell window (diameter 6 mm) and exposed to the aqueous electrolyte solutions. A platinum wire electrode and a Ag|AgCl (saturated KCl) electrode (BAS, Japan) were employed as counter and reference electrodes, respectively. The measurements were performed under anaerobic conditions in a dark box. The photocurrent response was recorded under potentiostatic conditions with exposure to the light under an N_2 atmosphere. The modified side of the electrode was irradiated by a 500 W xenon arc lamp (Ushio Optical Modulex, SX-U1501XQ) filtered with an IR cut-off filter (Asahi Spectra, Super cold filter 5C0751) or a monochromator (Shimadzu, SPG-120S). The electrode was placed at a distance of 20 cm from the edge of the guided optical fiber. The light intensity of the monochromatic light at the electrode surface was monitored with a luminometer (Minolta, Illuminance meter T-10P).

Received: July 24, 2011
Revised: September 16, 2011
Published online: October 6, 2011

Keywords: cytochromes · hemoproteins · host–guest systems · photochemistry · porphyrinoids

[1] a) I. Willner, E. Katz, *Bioelectronics*, Wiley-VCH, Weinheim, **2005**; b) L. Fruk, C. H. Kuo, E. Torres, C. M. Niemeyer, *Angew. Chem.* **2009**, *121*, 1578–1603; *Angew. Chem. Int. Ed.* **2009**, *48*, 1550–1574; c) L.-Y. Cheng, Y.-T. Long, H.-B. Kraatz, H. Tian, *Chem. Sci.* **2011**, *2*, 1515–1518.

[2] a) N. Terasaki, N. Yamamoto, T. Hiraga, Y. Yamanoi, T. Yonezawa, H. Nishihara, T. Ohmori, M. Sakai, M. Fujii, A. Tohri, M. Iwai, Y. Inoue, S. Yoneyama, M. Minakata, I. Enami, *Angew. Chem.* **2009**, *121*, 1613–1615; *Angew. Chem. Int. Ed.* **2009**, *48*, 1585–1587; b) M. Miyachi, Y. Yamanoi, Y. Shibata, H. Matsumoto, K. Nakazato, M. Konno, K. Ito, Y. Inoue, H. Nishihara, *Chem. Commun.* **2010**, *46*, 2557–2559.

[3] Y. Xiao, F. Patolsky, E. Katz, J. F. Hainfeld, I. Willner, *Science* **2003**, *299*, 1877–1881.

[4] a) A. Das, M. H. Hecht, *J. Inorg. Biochem.* **2007**, *101*, 1820–1826; b) H. Zimmermann, A. Lindgren, W. Schuhmann, L. Gorton, *Chem. Eur. J.* **2000**, *6*, 592–599; c) L. H. Guo, G.

McLendon, H. Razafitrimo, Y. L. Gao, *J. Mater. Chem.* **1996**, *6*, 369 – 374.

[5] a) I. Willner, E. Katz, *Angew. Chem.* **2000**, *112*, 1230 – 1269; *Angew. Chem. Int. Ed.* **2000**, *39*, 1180 – 1218; b) P. N. Ciesielski, F. M. Hijazi, A. M. Scott, C. J. Faulkner, L. Beard, K. Emmett, S. J. Rosenthal, D. Cliffel, G. K. Jennings, *Bioresour. Technol.* **2010**, *101*, 3047 – 3053; c) L. Frolov, O. Wilner, C. Carmeli, I. Carmeli, *Adv. Mater.* **2008**, *20*, 263 – 266; d) M. Lahav, T. Gabriel, A. N. Shipway, I. Willner, *J. Am. Chem. Soc.* **1999**, *121*, 258 – 259.

[6] a) H. Kitagishi, Y. Kakikura, H. Yamaguchi, K. Oohora, A. Harada, T. Hayashi, *Angew. Chem.* **2009**, *121*, 1297 – 1300; *Angew. Chem. Int. Ed.* **2009**, *48*, 1271 – 1274; b) H. Kitagishi, K. Oohora, T. Hayashi, *Biopolymers* **2009**, *91*, 194 – 200; c) H. Kitagishi, K. Oohora, H. Yamaguchi, H. Sato, T. Matsuo, A. Harada, T. Hayashi, *J. Am. Chem. Soc.* **2007**, *129*, 10326 – 10327; d) A. Onoda, Y. Ueya, T. Sakamoto, T. Uematsu, T. Hayashi, *Chem. Commun.* **2010**, *46*, 9107 – 9109.

[7] K. Oohora, A. Onoda, H. Kitagishi, H. Yamaguchi, A. Harada, T. Hayashi, *Chem. Sci.* **2011**, *2*, 1033 – 1308.

[8] a) M. M. C. Bastings, T. F. A. de Greef, J. L. J. van Dongen, M. Merkx, E. W. Meijer, *Chem. Sci.* **2011**, *2*, 79 – 88; b) J. C. Carlson, S. S. Jena, M. Flenniken, T. F. Chou, R. A. Siegel, C. R. Wagner, *J. Am. Chem. Soc.* **2006**, *128*, 7630 – 7638; c) S. Burazerovic, J. Gradinaru, J. Pierron, T. R. Ward, *Angew. Chem.* **2007**, *119*, 5606 – 5610; *Angew. Chem. Int. Ed.* **2007**, *46*, 5510 – 5514; d) D. A. Uhlenheuer, K. Petkau, L. Brunsveld, *Chem. Soc. Rev.* **2010**, *39*, 2817 – 2826; e) H. D. Nguyen, D. T. Dang, J. L. J. van Dongen, L. Brunsveld, *Angew. Chem.* **2010**, *122*, 907 – 910; *Angew. Chem. Int. Ed.* **2010**, *49*, 895 – 898.

[9] a) Y. Tokita, J. Shimura, H. Nakajima, Y. Goto, Y. Watanabe, *J. Am. Chem. Soc.* **2008**, *130*, 5302 – 5310; b) E. Topoglidis, C. J. Campbell, E. Palomares, J. R. Durrant, *Chem. Commun.* **2002**, 1518 – 1519; c) S. Takeda, N. Kamiya, T. Nagamune, *Biotechnol. Lett.* **2004**, *26*, 121 – 125; d) T. Matsuo, A. Asano, T. Ando, Y. Hisaeda, T. Hayashi, *Chem. Commun.* **2008**, 3684 – 3686; e) Y. Hitomi, T. Hayashi, K. Wada, T. Mizutani, Y. Hisaeda, H. Ogoshi, *Angew. Chem.* **2001**, *113*, 1132 – 1135; *Angew. Chem. Int. Ed.* **2001**, *40*, 1098 – 1101.

[10] a) H. Anni, J. M. Vanderkooi, L. Mayne, *Biochemistry* **1995**, *34*, 5744 – 5753; b) S. M. Tremain, N. M. Kostić, *Inorg. Chem.* **2002**, *41*, 3291 – 3301.

[11] ZnPPs **1a** and **1b** contain regioisomers with respect to the substitution position at the two heme propionate side chains of protoporphyrin IX.

[12] The surface concentration of the modified ZnPP was $1.7 \text{ mol} \times 10^{-12} \text{ mol cm}^{-2}$.

[13] The EIS experiment showed that the negatively charged ZnPP–apoCYT protein does not bind nonspecifically to the anionic surface of the SAM, which includes propionate groups.

[14] The maximum current (with clear photoresponses) was obtained under a bias potential of −200 mV (see the Supporting Information).

[15] The incident photon-to-current conversion efficiency was 0.061 %.

